describe phenomena that make determination of the appropriate boundary conditions relatively straightforward. However, the introduction of simultaneous heat and mass transfer with chemical reactions, phase changes, and velocity slip significantly complicates the situation. The conventional technique for obtaining boundary conditions involves placing a control volume around the boundary plane with subsequent application of appropriate global conservation principles. Quite often this procedure appears disconnected to the system of equations that are being solved and has led to incorrect results because of the absence of a uniformly consistent approach to the problem.

In lieu of applying overall conservation relations to the control volume that surrounds the boundary plane, it is possible to formally integrate the exact governing differential equations in the direction normal to the streamwise coordinate from a location $\epsilon/2$ below the plane to $\epsilon/2$ above it and let ϵ go to zero, assuming that the fluid equations hold throughout the region. Utilizing this procedure, the general multidimensional, nonsteady differential conservation equations result in the following "jump" (δ) conditions across the boundary plane of interest, in a manner identical to that applied to shock waves in Ref. 1

Continuity

$$\delta(\rho v) = 0 \tag{1}$$

Streamwise Momentum

$$\delta(\rho u v) = \delta\tau \tag{2}$$

Normal Momentum

$$\delta(\rho v^2) = -\delta p \tag{3}$$

Energy

$$\delta(\rho v E) - \delta(\tau u) + \delta(pv) + \delta(q_y) = 0 \tag{4a}$$

or

$$\delta(\rho v H) - \delta(\tau u) + \delta(q_y) = 0 \tag{4b}$$

where ρ is the local fluid density, and u, v are the streamwise and normal components of velocity, respectively. The elements of the stress tensor are represented by the static pressure p and the relevant component of shear stress τ. Transverse heat flux is contained in the term q_y whereas the potential energies of reaction or phase change are embedded in a generalized total energy E or enthalpy H.

When applying these conditions to a boundary of interest, it is apparent that any terms that are known to be continuous across it simply drop out of the equations. The resulting expressions provide the desired relationship between the behavior of the unknown terms and those that are being imposed on the solution of the particular problem.

The simplest of these expressions is provided by Eq. (1), which enforces the conservation of mass flux through the boundary plane while allowing both ρ and v to change across it. The streamwise momentum relationship presented in Eq. (2) dictates that the change in shear stress across the boundary is related to the velocity slip, since, as has been noted, ρv is conserved. In the case of flow along a solid boundary in which the zero slip condition is satisfied, the shear stress on the wall therefore is equal to the shear stress in the fluid at the wall, with or without mass transfer.

Conservation of normal momentum, as expressed in Eq. (3), introduces the possibility of a change in pressure across the boundary in the event that the normal velocity changes, for example, in the presence of mass transfer with a change of phase. Of prime importance, however, is the application of conservation of energy in the form of Eq. (4), which illustrates the fact that, without velocity slip or mass transfer (or with isoenthalpic mass transfer), the heat transfer in the fluid at the wall is equal to the wall heat transfer, which allows the respective temperature gradients to be related through Fourier's law. With the introduction of velocity slip, Eq. (4) expresses the relationship

$$q_{y_w} = q_{y_f} - \tau u \tag{5}$$

where a coordinate system at rest with respect to the wall has been utilized. In Eq. (5), τu represents the shear in the fluid at the wall and slip velocity, respectively, whereas the subscripts w and f refer to wall and flowfield quantities. Introduction of nonisoenthalpic mass transfer additionally complicates the energy balance such that Eq. (5) must be written as

$$q_{y_w} = q_{y_f} - \tau u + \delta(mH) \tag{6}$$

where $m \equiv \rho v$, and either or both of the mass transfer terms represent the sum of multiple phase transports, each with various heats of reaction or phase change.

The application of Eq. (6) to an external boundary plane (for example, at the edge of a condensing liquid wall layer being driven by a gas stream) is a situation in which some confusion might arise. Note that, in the true integral solution of the entire liquid film, the shear work term τu must be included explicitly in the energy balance; however, according to Eq. (4), the effect does not enter the external boundary condition evaluation, since both τ and u usually are continuous at the interface of the liquid and gas layers.

It is clear that other equations such as species conservation or extended versions of the basic equations presented here, with additional terms appropriate to specific situations, may be treated in an identical manner. In general, regardless of which equations are being evaluated with respect to boundary condition formulation, the virtue of the technique utilized here becomes apparent only in more complex situations. Although there is no current controversy regarding this problem, it is a fact that, in the past, the absence of a uniform approach to the specification of boundary conditions has resulted in some discrepancies[2-4] with regard to the appropriate form for the heat-transfer boundary condition with velocity slip. To the author's knowledge, the mechanism presented here has not been generally employed for this class of problems, and it is one that, especially for scientists who are being introduced to some of these peculiar and interesting phenomena, provides a significant degree of unity and coherence to the equation/boundary condition formulation.

Acknowledgment

The author would like to acknowledge the very helpful critique provided by F. E. C. Culick.

References

[1]Courant, R. and Friedrichs, K.O., *Supersonic Flow and Shock Waves*, Interscience, New York 1948, p. 136.

[2]Van Dyke, M., "Higher-Order Boundary-Layer Theory," *Annual Review of Fluid Mechanics*, Vol. 1, 1969, pp. 265-292.

[3]Maslen, S. H., "On Heat Transfer In Slip Flow," *Journal of Aeronautical Science*, Vol. 25, June 1958, pp. 400-401.

[4]Maslen, S.H., "Second-Order Effects In Laminar Boundary Layers," *AIAA Journal*, Vol. 1, Jan. 1963, pp. 33-40.

Bounds on the Dynamic Characteristics of Rotating Beams

T. J. McDaniel* and V. R. Murthy†
Iowa State University, Ames, Iowa

Introduction

THE dynamic characteristics of rotating beams find application in rotating machinery, helicopters, windmills,

Received July 31, 1975; revision received Aug. 19, 1976.
Index category: Structural Dynamic Analysis.

*Associate Professor, Dept. of Aerospace Engineering and Engineering Research Institute.

†Visiting Assistant Professor, Dept. of Aerospace Engineering, presently Visiting Assistant Professor, Old Dominion University, Norfolk, Virginia, Dept. of Mechanical Engineering and Mechanics.

etc. These characteristics, i.e., natural frequencies and mode shapes, are required to determine resonant responses and for forced vibration analyses. The present study presents a new approach based upon obtaining solution bounds to determine these characteristics.

The transfer matrix method which has been used in the dynamic analysis of a variety of structures[1-7] is well suited for the analysis of the rotating beams or blades. Since the beam has variable tension due to rotation and possibly variable twist or taper as a function of span, the governing equations of motion have variable coefficients in the spanwise coordinate. Solution of these equations in terms of known functions has not been obtained. Thus, a discretization of the rotating beam or numerical procedures such as the Runge-Kutta, predictor-corrector are used to obtain numerical transfer matrices. The accuracy of numerical transfer matrices or the discrete system representation is not known. Hence, the accuracy of the final numerical result cannot be determined. By constructing upper and lower bounds on the computations at each stage of the analysis, upper and lower bounds can be determined for the final solution. The theory of differential and integral inequalities provides a method of constructing such bounds.

The theory of differential and integral inequalities provides a method of constructing bounds to the solution for a wide range of engineering problems. The texts of Walter,[8] Protter and Weinberger,[9] and Lakshmikantham and Leela[10] summarize the major results and contain numerous references. The theory of differential inequalities applies primarily to differential equations of the initial value type. Since the transfer matrix method converts a two-point boundary-value problem to an initial value problem, the inequality theorems directly apply to linear structures with varying geometry. The inequality theorems have not been developed sufficiently to allow the construction of bounds to nonlinear boundary-value problems except for special classes of problems. It is also possible to construct bounds to the solution for certain types of partial differential equations, but in practice it is not a simple matter to construct useful bounds.

Until recently, few applications of the theory of differential inequalities have appeared in the engineering literature. The reasons are that application procedures are somewhat problem-dependent and that at least double the computations would be required. For the analysis of varying geometry beams Refs. 11 and 12 have developed procedures for obtaining and improving bounds. The accuracy of the final computation was judged by the number of places of agreement of the upper and lower bounds of the solution.

Application of Differential Inequalities

Differential inequalities are employed in this analysis to obtain bounds on the response characteristics of a uniform geometry rotating beam undergoing bending about one axis. When the beam undergoes simple harmonic motion with frequency ω, the governing equation for the undamped system can be written as a subcase of the equations derived in Ref. 13 in the form

$$\frac{d}{dx}[T(x)]=[A(x)][T(x)] \quad 0\le x\le \ell \tag{1}$$

with initial condition $[T(0)]=[I]$ where $[T(x)]$ is the transfer matrix for the beam. The matrix $[A(x)]$ is given by

$$[A(x)]=\begin{bmatrix} 0 & 1 & 0 & 0 \\ 0 & 0 & b & 0 \\ 0 & t(x) & 0 & 1 \\ m\omega^2 & 0 & 0 & 0 \end{bmatrix} \tag{2}$$

where

$$b = 1/EI$$

$$t(x)=\frac{\Omega^2 m}{2}(\ell^2-x^2)$$

The tension in the rotating beam $t(x)$ depends on the frequency of rotation Ω, the mass per unit length m, and the length of the blade ℓ. The section property $EI(x)$ can vary for the beam. In the absence of a closed-form solution we proceed to obtain bounds to this problem by denoting $[\hat{T}(x)]$ and $[\check{T}(x)]$ as the desired upper and lower bounds to $[T(x)]$. According to Ref. 8, the necessary conditions which $[\hat{T}(x)]\ge[T(x)]\ge[\check{T}(x)]$ holds in the interval $0\ge x\ge\ell$ are

$$\frac{d}{dx}[\hat{T}(x)]\ge[A(x)][\hat{T}(x)] \tag{3}$$

$$\frac{d}{dx}[\check{T}(x)]\le[A(x)][\check{T}(x)] \tag{4}$$

$$[\hat{T}(0)]\ge[I]\ge[\check{T}(0)] \tag{5}$$

Inequality is allowed in Eq. (5), but better bounds are obtained if strict equality is required. Approximate bounds are established by solving a constant coefficient differential equation. Assuming $EI(x)$ is also monotone nonincreasing in $0\le x\le\ell$ then $[A(x)]$ is set to its maximum value $[A(0)]$ and the equation (EI is assumed constant for following examples)

$$\frac{d[(\hat{x})]}{dx}=[A(0)][\hat{T}(x)] \tag{6}$$

subject to $[\hat{T}(0)]=[I]$ is solved. One can easily show, since all elements of $[T(x)]$ are nonnegative, that $[\hat{T}(x)]$ is an upper bound in the given interval. A similar procedure using the minimum value of $[A(x)]$, i.e., $[A(\ell)]$, in the interval $0\le x\le\ell$ results in a lower bound in that interval,

$$\frac{d[\hat{T}(x)]}{dx}=[A(\ell)][\check{T}(x)] \tag{7}$$

subject to $[\check{T}(0)]=[I]$. The solutions for the preceding equations are found in Ref. 1.

Now that rough bounds for the transfer matrix have been established for the rotating beam, these bounds can be used to obtain bounds on natural frequencies and mode shapes. Usually, these bounds will not be of sufficient accuracy to be of interest to the engineer. Two procedures for improving these bounds for the present analysis are compared in the following.

Improved Transfer Matrix Bounds

One procedure for improving the transfer matrix bounds is to use Eqs. (6) and (7) in small intervals so that the tension in the beam does not change signficantly. In Fig. 1 the blade tension curve is divided into N intervals and approximated by piecewise continuous upper and lower bound constant tension

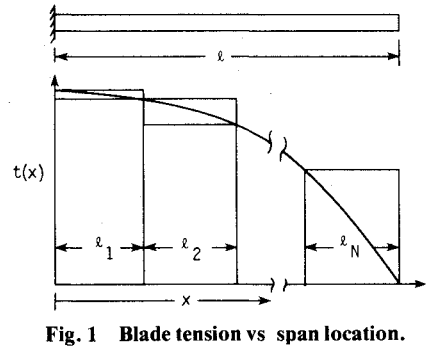

Fig. 1 Blade tension vs span location.

curves. If $[A(0)]$ and $[A(\ell_1)]$ are, respectively, inserted in Eqs. (6) and (7), the required transfer matrix bounds $[\hat{T}(\ell_1)]$, $[\tilde{T}(\ell_1)]$ for that interval are known. In the second interval the upper and lower bounds transfer matrices $[\hat{T}(\ell_2)]$, $[\tilde{T}(\ell_2)]$ are obtained by inserting $[A(\ell_1)]$ and $[A(\ell_2)]$, respectively, into Eqs. (6) and (7). Actually, the solution of Eq. (6) is not required as this upper bound transfer matrix was obtained in the previous interval as a lower bound transfer matrix, provided the intervals are the same length. The upper and lower bound transfer matrices over the entire interval $[\hat{T}]$ and $[\tilde{T}]$ are related to the transfer matrix bounds for segments by

$$[\hat{T}] = [\hat{T}_{(\ell_n)}] \ldots [\hat{T}_{(\ell_1)}] \tag{8a}$$

$$[\tilde{T}] = [T_{(\ell_n)}] \ldots [\tilde{T}01(\ell_n)]\,[\tilde{T}_{(\ell_n)}] \tag{8b}$$

The simple formula given in Eq. (8) results from the fact that all transfer matrix bounds are nonnegative.

The second procedure for improving the bounds is to develop an iteration procedure. By writing Eq. (1) with initial conditions Eq. (2) as an integral equation, one obtains

$$[T_{(x)}] = \int_0^x [A_{(y)}][T_{(y)}]\mathrm{d}y + [I] \tag{9}$$

Since $[A_{(y)}]$ contains nonnegative elements, it is clear that if the upper bound transfer matrix of Eq. (6) were inserted on the left-hand side of Eq. (9) the resulting $[T_{(x)}]$, which is denoted by $[\hat{T}_1(x)]$, would also be an upper bound.

It follows from differential inequalities that $[\hat{T}_1(x)]$ is a better upper bound. The term $[\hat{T}_1(x)$ can then be iterated to further improve the upper bound, i.e., to obtain $[\hat{T}_2(x)]$, $[\hat{T}_3(x)]$, etc. The same procedure can be used to develop the sequence of lower bounds starting with $[\hat{T}_1(x)]$ from Eq. (7) and using Eq. (9). The result is

$$[\hat{T}_1(x)] \geq [\hat{T}_2(x)] \geq [\hat{T}_3(x)] \ldots$$

$$\geq [T(x)] \geq \ldots [\tilde{T}_2(x)] \geq [\tilde{T}_1(x)] \tag{10}$$

This procedure can be accomplished analytically in the present case and thus reduces the computation to a minimum. The first procedure discussed in the preceding requires more computation but reduces the analytical work. These two methods are contrasted in the following in the computation of bounds on the natural frequencies and mode shapes of a rotating beam.

Bounds on Modes and Frequencies

To compute bounds on the natural frequencies of a rotating beam, the boundary conditions clamped and free were applied to the transfer matrix equation relating the root and tip of the beam. The resulting frequency determinant

$$\Delta(\omega) = t_{33}t_{44} - t_{34}t_{43} = 0$$

would be obtained if the t_{ij}'s were known. In terms of bounds,

$$\hat{\Delta}(\omega) = \hat{t}_{33}\hat{t}_{44} - \tilde{t}_{34}\tilde{t}_{43} = 0$$

$$\tilde{\Delta}(\omega) = \tilde{t}_{33}\tilde{t}_{44} - \hat{t}_{34}\hat{t}_{43} = 0$$

Since $\hat{\Delta}(0) \geq \tilde{\Delta}(0)$ and both are positive, the first zero of $\hat{\Delta}(\omega)$ and $\tilde{\Delta}(\omega)$ yield, respectively, upper and lower bounds to the first natural frequency. That is

$$\hat{\Delta}(\hat{\omega}_1) = 0 \qquad \tilde{\Delta}(\tilde{\omega}_1) = 0$$

yield

$$\hat{\omega}_1 \geq \omega_1 \geq \tilde{\omega}_1 \tag{11}$$

Because $\hat{\Delta}$ and $\tilde{\Delta}$ are ordered, one obtains at the second natural frequency

$$\tilde{\Delta}(\tilde{\omega}_2) = 0 \quad \tilde{\Delta}(\hat{\omega}_2) = 0 \text{ and thus } \hat{\omega}_2 \geq \omega_2 \geq \tilde{\omega}_2 \tag{12}$$

Additional frequencies are obtained by alternately using Eqs. (11) and (12).

As an application of the preceding, bounds on the natural frequencies of a model rotor blade were obtained using both procedures for obtaining transfer matrix bounds. The following blade data was used in the computations

Span of blade	ℓ	$=40.0$ in.
Mass per unit span	m	$=.0015$ slugs/in.
Bending stifnness	EI	$=25{,}000$ lb/in.^{2}
Rotational velocity	Ω	$=60.0$ rad/sec

The results are compared in Table 1 with Ref. 14, where the natural vibration characteristics were determined using the integrating matrix method and the transfer matrix methods using Runge-Kutta. To show the convergence of the bounds, upper and lower bounds are obtained when the blade is divided into 100 and 400 segments for modes 1, 2, and 3. Clearly, the agreement of the bounds increases with the number of segments and decreases with the mode number. Also given in Table 1 are the bounds which have been iterated twice in 100 and 600 segments of the blade. One can see that two iterations for 100 segments is slightly better than results obtained for 400 segments without iteration. The two iterations in 600 sections data shows that the Runge-Kutta results lie within the bounds, but the integrating matrix results are not within the bounds. One finds that for the upper and lower frequency bounds to agree to two or three signficant digits the transfer matrix bounds must agree to three or four significant digits.

Once bounds on the natural frequencies have been obtained, bounds can then be obtained for the corresponding mode shapes. The mode shape bounds are based upon the exact solution, which is unknown, having given amplitude at

Table 1 Bounds to natural frequencies (rad/sec)

Mode	100 Segments no iterations	400 Segments no iterations	100 Segments 2 iterations	600 Segments 2 iterations	Runge-Kutta	Integrating Matrix Method
1	73.2511 UB	71.9976 UB	71.5885 UB	71.5844 UB	71.5844	71.5853
	69.9434 LB	71.1761 LB	71.5803 LB	71.5844 LB		
2	252.9452 UB	248.8679 UB	247.5935 UB	247.4764 UB	247.4762	247.4778
	241.1811 LB	246.0951 LB	247.3500 LB	247.4752 LB		
3	618. 5136 UB	604.2740 UB	604.9564 UB	601.1260 UB	601.1136	601.1091
	584.7188 LB	596.1753 LB	597.4534 LB	601.0899 LB		

Table 2 Deflection bounds on modes 1 and 2

Station X/R	I Mode, 600 segments, 2 iterations UB	Runge-Kutta method	LB	II Mode, 600 segments, 2 iterations UB	Runge-Kutta method	LB
0.0	0.0000	0.0000	0.0000	0.0000	0.0000	0.0000
0.2	0.0871	0.0871	0.0871	−0.2878	−0.2888	−0.2898
0.4	0.2738	0.2738	0.2738	−0.6273	−0.6336	−0.6400
0.6	0.5023	0.5023	0.5023	−0.5144	−0.5393	−0.5641
0.8	0.7485	0.7485	0.7485	0.1759	0.0916	0.0072
1.0	1.000018	1.0000	0.999982	1.2648	1.0000	0.7352

some point on the structure. In the present case a unit tip amplitude of the rotor is specified. In terms of bounds on the transfer matrix elements, bounds on the deflection mode shape $W(x)$ are given by

$$\hat{W}(x) = \hat{t}_{13}\hat{t}_{34}/\hat{D} - \tilde{t}_{14}\tilde{t}_{33}/\hat{D} \text{ where } \hat{D} = \hat{t}_{13}\hat{t}_{34} - \tilde{t}_{14}\tilde{t}_{33}$$

$$\tilde{W}(x) = \tilde{t}_{13}\tilde{t}_{34}/\tilde{D} - \hat{t}_{14}\hat{t}_{33}/\tilde{D} \qquad \tilde{D} = \tilde{t}_{13}\tilde{t}_{34} - \hat{t}_{14}\hat{t}_{33}$$

and

$$\tilde{D} > 0 \tag{13}$$

Note that all upper bounds transfer matrices are evaluated at the upper bound frequency for that mode. Slightly different expressions obtained by using rules given in Ref. 12 are used for the mode shape if $\tilde{D}$ is negative. Bounds for modes 1 and 2 are compared with a Runge-Kutta solution in Table 2. Bounds on the preceding frequencies can also be obtained by a procedure given in Ref. 15, but the method does not provide bounds on the corresponding mode shape which one can obtain by the present approach.

Acknowledgment

This research was sponsored by the National Science Foundation under Grant GK-40589 and by the Iowa State University Engineering Research Institute.

References

[1]Pestel, E. C. and Leckie, F. A., *Matrix Methods in Elastomechanics*, McGraw-Hill, New York, 1963.

[2]Lin, Y. K., *Probablistic Theory of Structural Dynamics*, McGraw-Hill, New York, 1963.

[3]McDaniel, T. J. and Henderson, J. P., "Review of Transfer Matrix Vibration Analysis of Skin Stringer Structure," *The Shock and Vibration Digest*, Vol. 6, No. 1 (Part I), Vol. 6, No. 2 (Part II), 1974.

[4]Lin, Y. K. and McDaniel, T. J., "Dynamics of Beam-Type Periodic Structures," *Journal of Engineering for Industry*, Vol. 91, 1969, pp. 1133-1141.

[5]Murthy, V. R. and Pierce, G. A., "Effect of Phase Angle on Multibladed Rotor Flutter," to be published in *Journal of Sound and Vibration*.

[6]Murthy, V. R., "Dynamic Characteristics of Rotor Blades," to be published in *Journal of Sound and Vibration*.

[7]Murthy, V. R. and Nigam, N. C., "Dynamic Characteristics of Stiffened Rings by Transfers Matrix Approach," *Journal of Sound and Vibration*, Vol. 39, No. 2, March 1975, pp. 237-245.

[8]Walter, W., *Differential and Integral Inequalities*, Springer-Verlag, New York, 1970.

[9]Protter, M. H. and Weinberger, H. S., *Maximum Principles in Differential Equations*, Prentice-Hall, Englewood Cliffs, New Jersey, 1967.

[10]Lakshmikantham, V., and Leela, S., *Differential and Integral Inequalities*, Vol. 1, *Ordinary Differential Equations*, Academic Press, New York and London, 1969.

[11]McDaniel, T. J. and Murthy, V. R., "Solution Bounds for Varying Geometry Beams," to appear in the *Journal of Sound and Vibration*.

[12]Murthy, V. R. and McDaniel, T. J., "Solution Rounds to Structural Systems," *AIAA Journal*, Vol. 14, Jan. 1976, pp. 111-113.

[13]Hubolt, J. C. and Brooks, G. W., "Differential Equations of Motion for Combined Flapwise Bending, Chordwise Bending, and Torsion of Twisted, Non-Uniform Rotor Blades," NASA Rep. 1346, 1958.

[14]Murthy, V.R., "Determination of Structural Dynamic Characteristics of Rotor Blades and the Effect of Phase Angle on Multi-bladed Rotor Flutter," Ph.D. dissertation, Georgia Institute of Technology, 1974.

[15]Bazley, N. W. and Fox, D. W., "Lower Bounds to Eigenvalues Using Operated Decompositions of the Form B*B," *Archive for Rational Mechanics and Analysis*, Vol. 10, 1962, pp. 352-360.

Rocket Nozzle Damping Characteristics Measured Using Different Experimental Techniques

B. A. Janardan* and B. T. Zinn†
Georgia Institute of Technology, Atlanta, Ga.

Introduction

In linear stability considerations of rocket motors, it is customary to evaluate the effect of the nozzle on the growth or decay rate of a small-amplitude oscillation inside the combustor by determining the nozzle decay coefficient. When the nozzle is the only factor that affects the combustor oscillation, the temporal behavior of the oscillation in terms of the nozzle decay coefficient α_N can be expressed in the following form:

$$P_1(z,t) = P(z)e^{(\alpha_N t)}e^{(i\omega t)}$$

To date, several experimental techniques have been developed for the determination of the values of α_N of rocket nozzles. It is the objective of this investigation to determine the decay coefficient α_N of a small-scale solid rocket exhaust nozzle by all of the available experimental methods and to compare the data so obtained with one another and with available empirical and theoretical nozzle damping data. The measured data are presented in this note, together with a brief review of the techniques used to measure α_N.

Experimental Techniques

An apparatus commonly employed to measure the rocket nozzle damping data is illustrated in Fig. 1. It consists of a simulated cold flow chamber with the test nozzle at one end and an injector plate at the other end. Using this apparatus, the nozzle damping characteristics have been measured employing several techniques.[1-4] These are referred to as the wave-attenuation, frequency-response, and standing-wave methods. These methods are reviewed briefly below, together with a discussion on their applicability for the determination of α_N.

Received Nov. 16, 1976.

Index categories: Combustion Stability, Ignition, and Detonation; Solid and Hybrid Rocket Engines.

*Research Engineer, School of Aerospace Engineering.

†Regents' Professor of Aerospace Engineering. Associate Fellow AIAA.